

# Molecular Staples for Tough and Stretchable Adhesion in Integrated Soft Materials

Baohong Chen, Jiawei Yang, Ruobing Bai, and Zhigang Suo\*

The integration of soft materials—biological tissues, gels, and elastomers—is a rapidly developing technology of this time. Whereas hard materials are adhered using adhesives of hard polymers since antiquity, these hard polymers are generally unsuited to adhere soft materials, because hard polymers constrain the deformation of soft materials. This paper describes a design principle to use hard polymers to adhere soft materials, such that adhesion remains tough after the adhered soft materials are subject to many cycles of large stretches in the plane of their interface. The two soft materials have stretchable polymer networks, but need not have functional groups for adhesion. The two soft materials are adhered by forming, *in situ* at their interface, islands of a hard polymer. The adhesion is tough if the islands themselves are strong, and the polymers of the islands are in topological entanglement with the polymer networks of the soft materials. The adhesion is stretchable if the islands are smaller than the flaw sensitivity length. Several methods of forming the hard polymer islands are demonstrated, and the mechanics and chemistry of adhesion are studied. The design principle will enable many hard polymers to form tough and stretchable adhesion between soft materials.

## 1. Introduction

Existing and emerging applications of integrated soft materials are far-reaching, numerous, and diverse.<sup>[1–3]</sup> Examples include soft composites,<sup>[4–6]</sup> washable active textiles,<sup>[7]</sup> stretchable seals,<sup>[8]</sup> wound closure,<sup>[9–11]</sup> drug delivery,<sup>[12]</sup> synthetic biology,<sup>[13–15]</sup> soft robots,<sup>[3,16–19]</sup> ionotronics,<sup>[17,20]</sup> bioelectronics,<sup>[21]</sup> and human–machine interfaces.<sup>[22–24]</sup> A fundamental requirement common to most applications calls for immediate action: invent methods to achieve tough and stretchable adhesion between soft materials.

By comparison, hard materials (e.g., glass, wood, ceramic, and metal) can be bonded by adhesives such as epoxy, cyanoacrylate, and poly(vinyl acetate), each of which has been refined over a long history of development.<sup>[25]</sup> Such an adhesive comes as a liquid and, after applied between two adherends, forms a hard polymer.<sup>[26]</sup> The hard polymer withstands high stress, but

needs little deformation. These adhesives, however, are in general unsuited to adhere soft materials, because the hard polymers constrain the deformation of the soft materials.

Last few years have seen transformative advances in achieving tough and stretchable adhesion between soft materials. Reported methods include surface modification,<sup>[27]</sup> surface initiation,<sup>[28]</sup> bulk modification,<sup>[29]</sup> bulk initiation,<sup>[30]</sup> bridging polymers,<sup>[9]</sup> and topological adhesion.<sup>[31–33]</sup> As a prerequisite for tough and stretchable adhesion, each adherend is a tough and stretchable material, typically having at least one covalent polymer network. These methods adhere two soft materials by forming strong, but sparse, connection. Some of these methods form sparse covalent bonds *in situ*, interlinking the covalent polymer networks of the two soft materials. Other methods form noncovalent complexes *in situ*, in topological entanglement with

the covalent polymer networks of the adherends. Whereas both sparse covalent interlinks and topological adhesion have long achieved tough and stretchable adhesion between dry elastomers,<sup>[34,35]</sup> the development of these methods for wet soft materials (i.e., synthetic hydrogels and biological tissues) is recent. The recent advances expand the scopes of these methods, enabling tough and stretchable adhesion between various pairs: tissue–tissue, tissue–hydrogel, tissue–elastomer, hydrogel–elastomer, hydrogel–hydrogel, in addition to elastomer–elastomer.

Because of the enormous variety of soft materials, applications, and operations (attach, cast, print, coat, brush, and spray), the field remains wide open for inventing methods of tough and stretchable adhesion.<sup>[2]</sup> The covalent interlinks require complementary functional groups from the adherends, and the formation of some of these covalent interlinks requires toxic agents and special processing conditions. The noncovalent topological adhesion is tough and stretchable, but detaches easily in response to environmental stimuli, an attribute which can be either useful or limiting.<sup>[32,33]</sup>

A recent work shows that cyanoacrylates (commonly known as superglues), once diluted in an organic solvent and spread between two soft materials, can form tough and stretchable adhesion between the two soft materials.<sup>[36]</sup> Even though the mechanism of this tough and stretchable adhesion is unclear, its implication is important. In addition to adhering hard polymers, cyanoacrylates have long been used

B. Chen, Dr. J. Yang, Dr. R. Bai, Prof. Z. Suo  
John A. Paulson School of Engineering and Applied Sciences  
Kavli Institute for Bionano Science and Technology  
Harvard University  
MA 02138, USA  
E-mail: suo@seas.harvard.edu

 The ORCID identification number(s) for the author(s) of this article can be found under <https://doi.org/10.1002/adhm.201900810>.

DOI: 10.1002/adhm.201900810

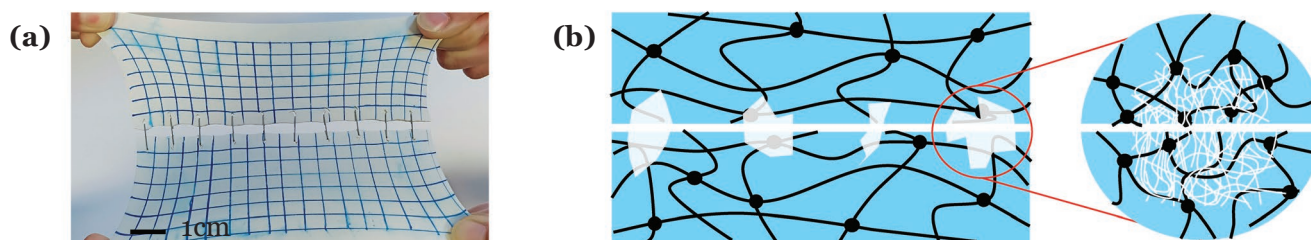


**Figure 1.** Steel staples and molecular staples. a) Steel staples connect two sheets of rubber, which resist separation, but remain stretchable. The deformation is shown by a square grid marked on the surface of each sheet. b) Molecular staples are islands of a hard polymer, formed in situ, in topological entanglement with the polymer networks of the two adherends. The two adherends have stretchable polymer networks, but do not have functional groups for adhesion. (White regions: solid polymers. Black and white lines: polymer chains. Black dots: crosslinkers of adherends.) The adhesion is tough because the hard islands resist separation of the adherends, and is stretchable because the hard islands allow deformation of the adherends at the scale larger than the individual staples.

in medicine to adhere soft tissues. Examples include emergent hemostasis, traumatic wound dressing, and skin closure.<sup>[37–39]</sup> The medical concerns for cyanoacrylates are well known. In addition to forming a glassy phase that constrains the deformation of soft tissues, cyanoacrylates are cytotoxic. The toxicity, however, is mitigated for cyanoacrylates having longer alkyl groups, such as the FDA-approved butyl- or octyl-cyanoacrylate.<sup>[37,40–42]</sup> The recent finding of tough and stretchable adhesion using cyanoacrylates raises an intriguing question. Can some of the cyanoacrylates, as well as other hard polymers, be recruited to achieve tough and stretchable adhesion, without toxicity?

Here we describe a design principle to integrate soft materials using hard polymers. We are inspired by steel staples, which can firmly connect two sheets of rubber, and allow the rubber to be stretchable at the scale larger than the individual staples (Figure 1a). We propose that the staples can be small islands of a hard polymer, formed in situ, in topological entanglement with the polymer networks of the two soft materials (Figure 1b). We call these hard polymer islands molecular staples. The adhesion is tough if the strength of the molecular staples is comparable to the polymer networks of the adherends, and is stretchable if the molecular staples are smaller than the flaw sensitivity length.

We demonstrate the design principle of molecular staples using several hard polymers and soft adherends. We form the molecular staples in topological entanglement with the polymer networks of the soft adherends in three ways: crack a continuous layer of the hard polymer cast at the interface into islands, print drops of the precursor, and spray drops of the precursor. We can form the molecular staples with either a diluted or an undiluted cyanoacrylate, as well as other adhesives. We confirm that topological entanglement occurs. Making adhesion both tough and stretchable was a relatively unusual requirement before the recent surge in developing integrated soft materials for diverse applications. We are unaware of any existing procedure to characterize tough and stretchable adhesion. Here we propose a procedure: measure adhesion energy *after* the adhered sample is subject to some cycles of large stretch in the plane of the interface. We demonstrate that the island-stapled soft materials can have high adhesion energy even after one thousand cycles of stretch.

## 2. Staple Two Hydrogels Using an Undiluted Cyanoacrylate

We use two polyacrylamide (PAAm) hydrogels as model soft materials with covalent polymer networks, but without functional groups for adhesion. We staple the two polyacrylamide hydrogels using an undiluted commercial glue based on ethyl-cyanoacrylate. Such a glue has small amounts of additives, including a thickener (e.g., poly(methyl methacrylate)) to adjust rheology, an inhibitor (e.g., sulfonic acid) to suppress anionic polymerization, and a stabilizer (e.g., phenol) to stabilize free radicals. When the glue is applied at the interface of the two hydrogels, the additives protect the cyanoacrylate monomers from rapid polymerization, and the monomers diffuse into both hydrogels. The additives and monomers become diluted by the abundant water in the hydrogel, and the monomers link into polycyanoacrylate chains through anionic polymerization (Figure 2).<sup>[43–45]</sup> Through the dipole–dipole interaction between the cyano (–CN) groups, the polycyanoacrylate chains aggregate into a glassy phase.<sup>[46]</sup> The glass transition temperature of polycyanoacrylate of various side groups lies in the range of 50–120 °C.<sup>[47]</sup> We hypothesize that during this concurrent diffusion, polymerization, and aggregation, the glassy polycyanoacrylate is in topological entanglement with the two polymer networks of the hydrogels. We will test this hypothesis in Section 3.

The diffusion length of the commercial formulation of cyanoacrylate into a hydrogel is reported to be  $L \approx 10 \mu\text{m}$  in the recent work using Raman spectroscopy.<sup>[36]</sup> We speculate that this length is related to the time period when the concentration of inhibitor in the glue falls below a critical value. Considering the diffusivity of small molecules in water  $D \approx 10^{-10} \text{ m}^2 \text{ s}^{-1}$ , we estimate the time period from the start of diffusion to the formation of glassy phase to be  $\tau = L^2/D \approx 1 \text{ s}$ . This time is consistent with our own observations of the time needed for the cyanoacrylate to form white color when it is applied on the surface of a hydrogel.

Several other lengths are significant. The mesh size of the polymer networks of the adherends is  $\approx 10 \text{ nm}$ . To form efficient adhesion, the size of island should be larger than the mesh size. If the size of the islands is below the wavelength of light, the adhesive layer becomes optically transparent. When two adherends are placed in contact, gaps inevitably exist at their

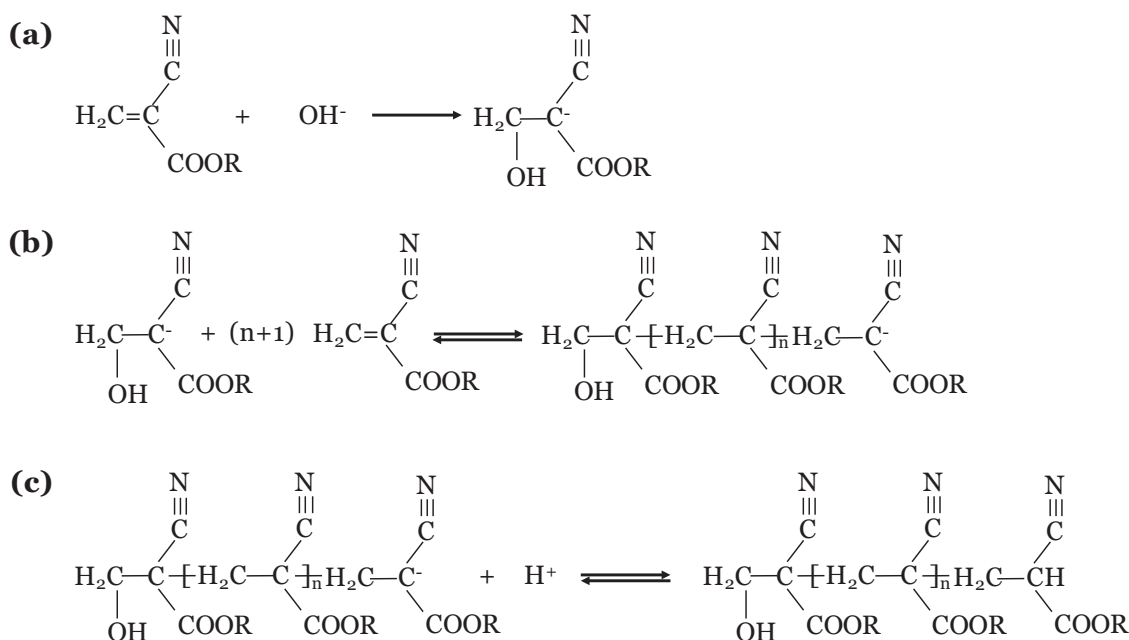


**Figure 2.** The anionic polymerization of cyanoacrylate. a) The hydroxide ion in water reacts with the cyanoacrylate monomer, makes it anionic, and initiates the polymerization. b) The cyanoacrylate monomers link into a polycyanoacrylate chain. c) The chain is terminated by a proton.

interface. The adherends under current study have low modulus ( $\approx 1$  kPa) and readily deform elastically to fill the gaps,<sup>[48]</sup> so we do not study the effect of the gaps. Of particular significance is the flaw sensitivity length, which is  $\approx 1$  mm for the polyacrylamide hydrogels.<sup>[49]</sup> An individual staple is regarded as a flaw in the hydrogels. If the size of the staple is larger than the flaw sensitivity length, the soft bilayer may form tough adhesion, but loses stretchability, because the large islands concentrate stress and cause the adherends to rupture at a small stretch. If the size of the staple is smaller than the flaw sensitivity length, the stretchability of the bilayer is insensitive to the presence of the staples. The hydrogels between the staples provide stretchability.

### 3. Tough Adhesion

#### 3.1. Evidence of Topological Entanglement

To verify the topological entanglement between the polycyanoacrylate and two polyacrylamide hydrogels, we measure the adhesion energy due to a continuous layer of the glassy polycyanoacrylate covering the entire interface. We conduct the 180° peel test at various peel velocities (Figure 3a). We fix an inextensible polyester back layer on the outward surface of each hydrogel, so that the active deformation in each hydrogel during peel is confined within a volume of  $\approx WH^2$  around the peel front, where  $W$  and  $H$  are the width and thickness of the hydrogel.<sup>[50]</sup> When the crack propagates in a steady state, the recorded force reaches a plateau  $F$ , giving the adhesion energy  $G = 2F/W$ .<sup>[51]</sup> In the steady state, the peel velocity  $V$  equals one half of the loading speed of the tensile machine. The measured adhesion energy is in the range of 250–400 J m<sup>-2</sup>, decreasing with the peel velocity (Figure 3c). For comparison, we also measure the

fracture energy of the polyacrylamide hydrogel itself using the same setup (Figure 3b). The fracture energy is in the range of 200 to 350 J m<sup>-2</sup> (Figure 3c). The excess of the measured adhesion energy compared to the fracture energy of the hydrogel is possibly caused by the additional toughening from bending and breaking the glassy polycyanoacrylate at the peel front. At a vanishingly low peel velocity, the adhesion energy approaches a threshold of about 250 J m<sup>-2</sup>. This threshold is much higher than the typical threshold of noncovalent adhesion, which is typically on the order of 1–10 J m<sup>-2</sup>.<sup>[2,52–54]</sup> We further measure the adhesion energies between polyacrylamide hydrogels with different concentrations of crosslinkers, and their corresponding fracture energies (Figure 3d). More crosslinkers correspond to smaller mesh size of a hydrogel. In all cases, the adhesion energy is comparable to the fracture energy of the adherend, and they both decrease as the concentration of crosslinkers increases.

In all peel tests conducted here, the crack propagates into one of the adherends and leaves a thin layer of the hydrogel on the polycyanoacrylate (Video 1). This observation again confirms that the peel causes decohesion of the polyacrylamide hydrogel, rather than the polycyanoacrylate. These measurements and observations are consistent with the hypothesis that the tough adhesion comes from the topological entanglement between the polycyanoacrylate and the polyacrylamide networks of the two adherends.

#### 3.2. Kinetics of Entanglement

To study the kinetics of entanglement, we spread the commercial formulation of cyanoacrylate on one piece of hydrogel, and immediately cover another hydrogel on top with a constant weight. We wait for a specified time and then measure the

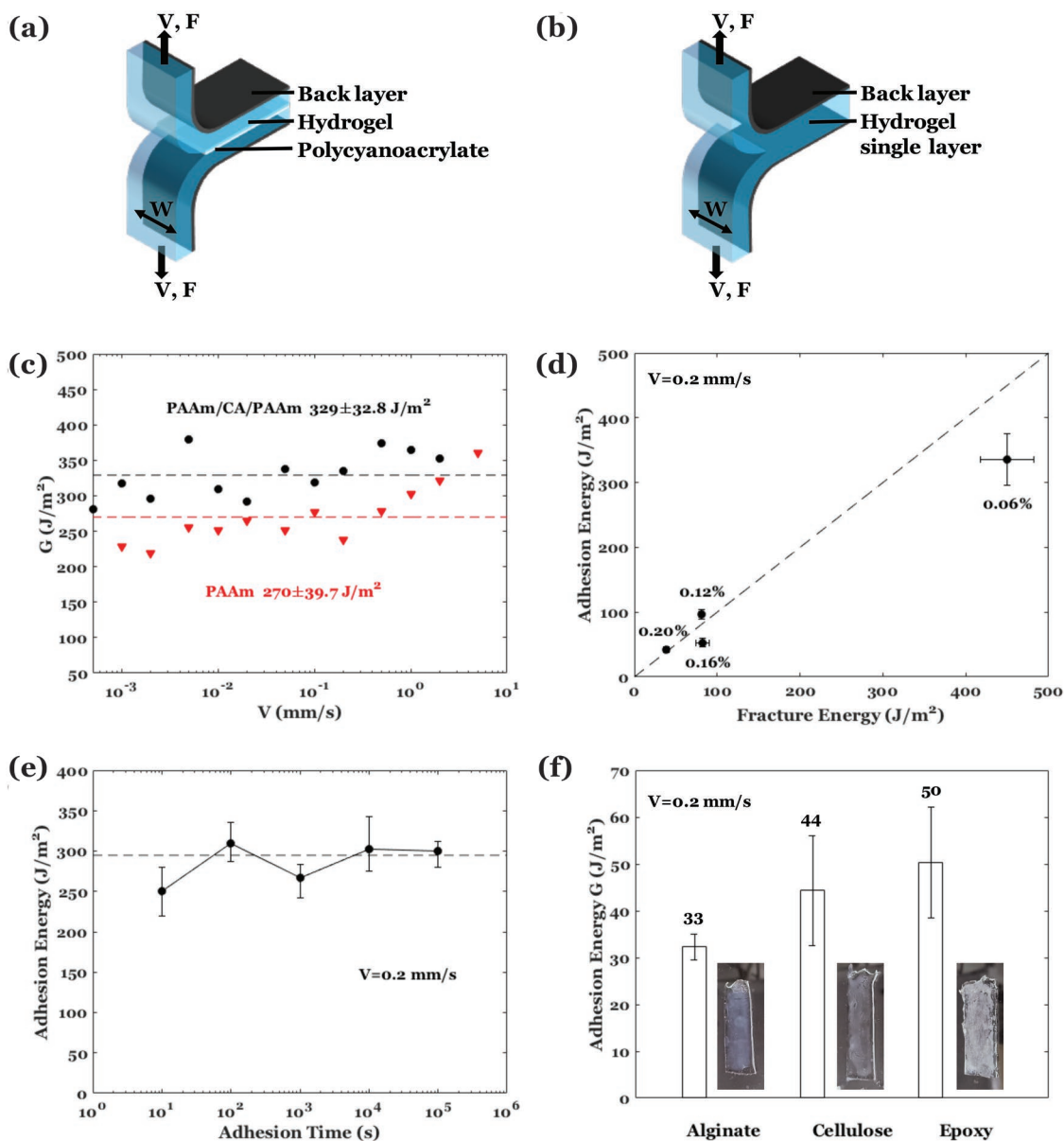


**Figure 3.** Tough adhesion by topological entanglement. a) Adhesion energy is measured by peeling two polyacrylamide hydrogels adhered by a continuous layer of polycyanoacrylate (CA) formed in situ. Inextensible back layers are attached on the surfaces of the hydrogels. b) Fracture energy is measured by peeling a polyacrylamide hydrogel. c) The adhesion energy and the fracture energy, both denoted as  $G$ , measured as functions of the peel velocity  $V$ . d) The adhesion energy approximately equals the fracture energy of the hydrogel, both decreasing with the increase of concentration of crosslinkers (indicated by the weight percentage to the monomer). e) The adhesion energy maintains nearly the same value after a time from seconds to hours. f) The adhesion energy of alginate, cellulose, and epoxy between two polyacrylamide hydrogels. The pH of the hydrogel is tuned to be 1, 5, and 7, respectively. Inset photos show the top view of the hydrogel after the adhesive solution is introduced on surface. The adhesion energies in (d)–(f) are measured at a peel velocity of  $0.2 \text{ mm s}^{-1}$ . All the data represent the mean of  $n \geq 3$  individual measurements. The standard deviations are labeled or represented by error bars.

adhesion energy. The adhesion energy is about  $250 \text{ J m}^{-2}$  after 1 min at a peel speed of  $0.2 \text{ mm s}^{-1}$ . The adhesion energy is almost unchanged with longer waiting time (Figure 3e). Therefore, the topological entanglement by in situ polymerization of cyanoacrylate is instant.

By contrast, we test the adhesion formed by several species of long-chain polymers. We prepare alginate and cellulose solutions as adhesives and synthesize polyacrylamide hydrogels

with different pH as adherends. Alginate ( $\text{pK}_a = 3.5$ ) and cellulose ( $\text{pK}_a = 13$ ) chains precipitate in a solution when the pH of the solution is lower than their  $\text{pK}_a$ . When diffusing into a hydrogel, the alginate or cellulose chains form topological entanglement with the hydrogel network.<sup>[32]</sup> We spread alginate and cellulose solutions on the hydrogels with  $\text{pH} = 1$  and 5, respectively, and cover another piece of the same hydrogel on top with a constant weight. Almost no adhesion is measured



if the waiting time is 1 min. The adhesion builds up to 30 to 45 J m<sup>-2</sup> after 1 h (Figure 3f). The hydrogels are nearly intact after peel, with some precipitated residuals on the surface. We suspect that the slow diffusion of the long-chain polymers in the hydrogel network results in the weaker cohesion of the precipitates of alginate and cellulose.

We also spread a commercial epoxy adhesive between two polyacrylamide hydrogels of pH = 7. The curing time of epoxy is around several tens of minutes,<sup>[55]</sup> much longer than the anionic polymerization of cyanoacrylate. This makes the adhesion negligible after the waiting time of 1 min. The adhesion energy is 50 J m<sup>-2</sup> after 1 h (Figure 3f). After peel, the hydrogels are intact, with no observable residuals of epoxy left on the surface of one of the hydrogels. It is possible that the epoxy does not diffuse much into the hydrogels before solidification. Topological entanglement between the epoxy and polyacrylamide hydrogel is poorly formed.

### 3.3. Adhesion without Topological Entanglement

Without topological entanglement, polycyanoacrylate and polyacrylamide hydrogel interact through sparse, noncovalent interaction, leading to brittle adhesion. To test this, we cast a film of cyanoacrylate monomers in a mold made of polydimethylsiloxane (PDMS) and then allow complete polymerization of the cyanoacrylate. Afterward, we cast the precursor of polyacrylamide hydrogel on top of the glassy polycyanoacrylate film, and let the hydrogel polymerize (Figure 4a). We measure the G–V curve using 90° peel tests (Figure 4b). In the steady state, the peel velocity *V* equals the loading speed of the tensile machine. The adhesion energy is in the range of 5–30 J m<sup>-2</sup> (Figure 4c), much lower than the adhesion energy achieved by forming the polycyanoacrylate in situ between the hydrogels (≈250 J m<sup>-2</sup>). Without being able to diffuse into the hydrogel network and subsequently polymerize, the polycyanoacrylate does not form topological entanglement with the polyacrylamide network. The weak adhesion is due to the sparse noncovalent bonds formed between the polycyanoacrylate and the polyacrylamide.

### 3.4. Adhesion Amplified by Bulk Dissipation

The adhesion energy can be further amplified by eliciting dissipation from the bulk of the adherends.<sup>[27]</sup> We confirm this effect for molecular staples using the calcium-alginate-polyacrylamide hydrogel.<sup>[56]</sup> The hydrogel has a covalent polyacrylamide network, in topological entanglement with a calcium-alginate complex. We adhere two pieces of the hydrogels by forming polycyanoacrylate in situ, in topological entanglement with the polyacrylamide networks of the hydrogels. When an applied force separates the adhesion, the polycyanoacrylate bridges the crack, transmits the intense stress from the front of the crack to the bulk of the hydrogels, and unzips a large volume of the calcium-alginate complex (Figure 5a). The adhesion energy is 1000 to 3000 J m<sup>-2</sup> for peel velocity from 5 × 10<sup>-4</sup> to 2 mm s<sup>-1</sup> (Figure 5b). The adhesion energy is one order of magnitude higher than that of a single-network polyacrylamide hydrogel.

The threshold for the polycyanoacrylate bonded calcium-alginate-polyacrylamide hydrogels is about 1000 J m<sup>-2</sup>. This threshold is comparable to the threshold for static fatigue crack growth of the calcium-alginate-polyacrylamide hydrogel itself,<sup>[50]</sup> and is much larger than the threshold of the single-network polyacrylamide hydrogel or other physically crosslinked hydrogels such as gelatin and alginate.<sup>[32,52,53]</sup> The large threshold again indicates that the tough adhesion is not merely due to a single layer of interlinking polymer chain or noncovalent interchain interaction, but is contributed both by the scission polyacrylamide chains at the separation and by the unzip of the calcium-alginate complex in the bulk of the hydrogels. See our recent reviews on the fatigue and adhesion of hydrogels.<sup>[2,54]</sup>

## 4. Stretchable Adhesion

While a continuous layer of glassy polycyanoacrylate can form tough adhesion between two hydrogels, it restricts the deformation of the hydrogels. When the adhered hydrogels are

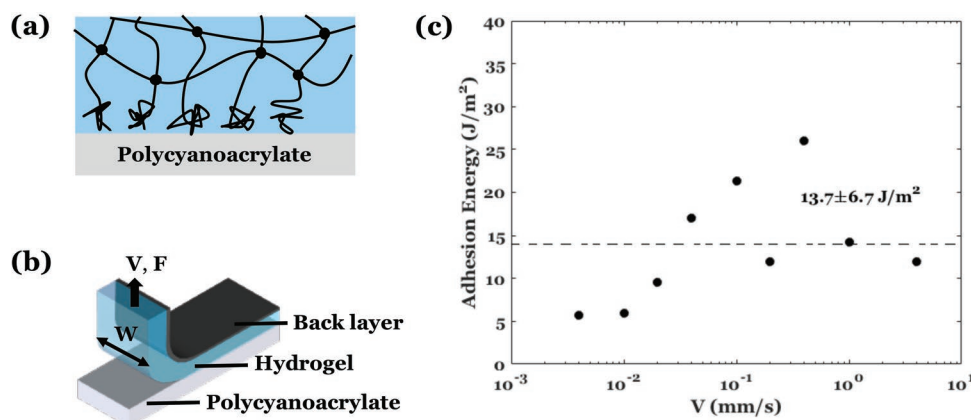


**Figure 4.** A hydrogel cast on a preformed glassy polycyanoacrylate film adheres weakly. a) A preformed polycyanoacrylate interacts with the hydrogel network only through sparse noncovalent bonds at the interface. b) The 90° peel test to measure the adhesion energy. c) The adhesion energy is on the order of 10 J m<sup>-2</sup> at all peel velocities, two orders of magnitude lower than the adhesion energy achieved by polycyanoacrylate formed in situ. The average adhesion energy is plotted as the dashed line and labeled by the mean value and the standard deviation.

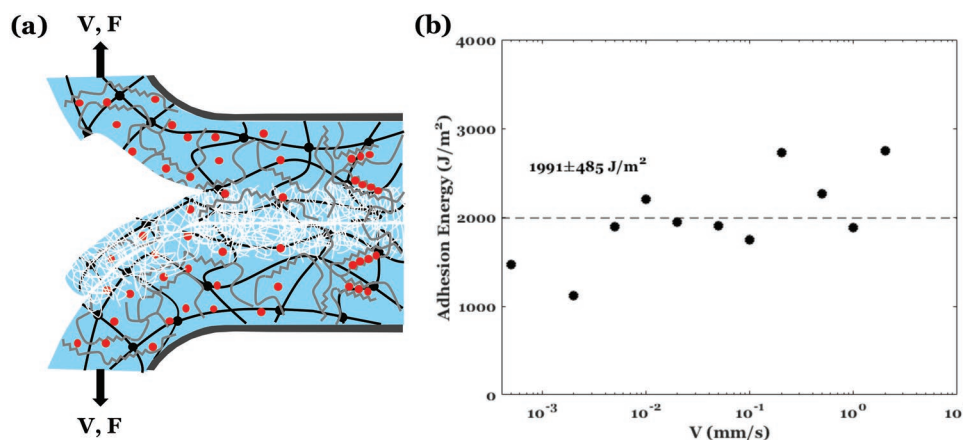


**Figure 5.** The adhesion energy is amplified by eliciting the dissipation from the bulk of the adherends. a) Schematic illustration of peeling two calcium-alginate-polyacrylamide hydrogels adhered by a continuous layer of polycyanoacrylate. (Gray lines: alginate chains. Red dots: calcium cations. Gray regions: back layers). b) The adhesion energy exceeds  $1000 \text{ J m}^{-2}$  at all peel velocities. The average adhesion energy is plotted as the dashed line and labeled by the mean value and the standard deviation.

stretched in the plane of the interface, the glassy layer ruptures at a relatively small stretch (Figure 6a).

#### 4.1. Hard Islands

Instead of the continuous hard layer, we can make small hard islands to achieve tough and stretchable adhesion. As discussed before, when the size of the individual islands is  $\approx 1 \text{ mm}$  or below, the polyacrylamide hydrogel bilayer is expected to be stretchable. To verify this, we evenly print drops of the cyanoacrylate of 1–2 mm diameter at the interface of two polyacrylamide hydrogels, and let them polymerize into glassy islands, in topological entanglement with the polymer networks of the hydrogels (Figure 6b). The size of printed island mainly depends on the tip size of lattice, and may also be affected by the wettability of adhesives on the surface of the hydrogel. Islands with other size and shape can be printed by prescribed tips of lattice. The adhered bilayer is subject to 100 cycles of stretch with an amplitude of 2 (Video 2). The force–displacement curve shows small hysteresis and good reversibility, similar to the polyacrylamide hydrogel itself. As the size of the glassy island further scales down, we expect that the stretchability of the bilayer is limited by the stretchability of the hydrogels, rather than the inextensible glassy islands.

While printing islands by manual operations is slow, inaccurate, and inefficient, nevertheless, incorporated in 3D printing or lithography, it is suitable to generate precise and elaborated islands of controlled size, shape, and spacing, which could be important to meet practical needs in certain applications. Printing is compatible with both nonsticky liquid adhesives and viscous adhesives. The strength of adhesion can be controlled by the density of printed islands. However, printing small islands is not very efficient in large scale adhesion.

For the calcium-alginate-polyacrylamide hydrogels, the flaw sensitivity length is  $\approx 10 \text{ cm}$ .<sup>[54]</sup> This estimate again agrees qualitatively with our experimental observation (Figure 6c). A continuous layer of the glassy polycyanoacrylate between a bilayer

of calcium-alginate-polyacrylamide hydrogels is fractured into pieces of  $\approx 1\text{--}2 \text{ cm}$  during the first cycle of stretch. Because the adherends are relatively tough, the glassy adhesive layer does not fracture the adherends during the stretch. The adhered bilayer becomes stretchable after the first cycle, and maintains the stretchability up to a stretch of 2 for 100 cycles (Video 3). The force–displacement curve shows large hysteresis in the initial loading cycle, and subsequent softening over many cycles, consistent with what was observed in the calcium-alginate-polyacrylamide hydrogel itself.<sup>[57]</sup>

In general, one can form a continuous layer of a brittle polymer, in topological entanglement with the polymer networks of two soft materials. So long as the brittle polymer and the two soft materials have suitable materials properties, the first cycle of stretch in the plane of the interface will break the brittle layer into islands without rupturing the soft materials, and the subsequent cycles of stretch will be nearly unconstrained by the presence of the brittle polymer. The “self-assembled” islands enable tough and stretchable adhesion.

#### 4.2. Characterization of Stretchable Adhesion

We propose and conduct a test to characterize tough and stretchable adhesion. We stretch a bilayer by a uniaxial force, in the plane of the interface, for many cycles of a fixed stretch amplitude of 2. Afterward, we measure the adhesion energy using the  $180^\circ$  peel test (Video 4). For both polycyanoacrylate-island-stapled polyacrylamide hydrogels and calcium-alginate-polyacrylamide hydrogels, adhesion remains tough even after 1000 cycles of prestretch (Figure 6d). The adhesion energy of the polyacrylamide bilayer only reduces slightly after 1000 cycles. The adhesion energy of the calcium-alginate-polyacrylamide bilayer reduces to approximately  $2/3$  of the initial value after 1000 cycles, still much higher compared to the polyacrylamide bilayer. The more reduction of the adhesion energy in the calcium-alginate-polyacrylamide bilayer is possibly because the cyclic prestretch unzips some of the calcium-alginate complex.

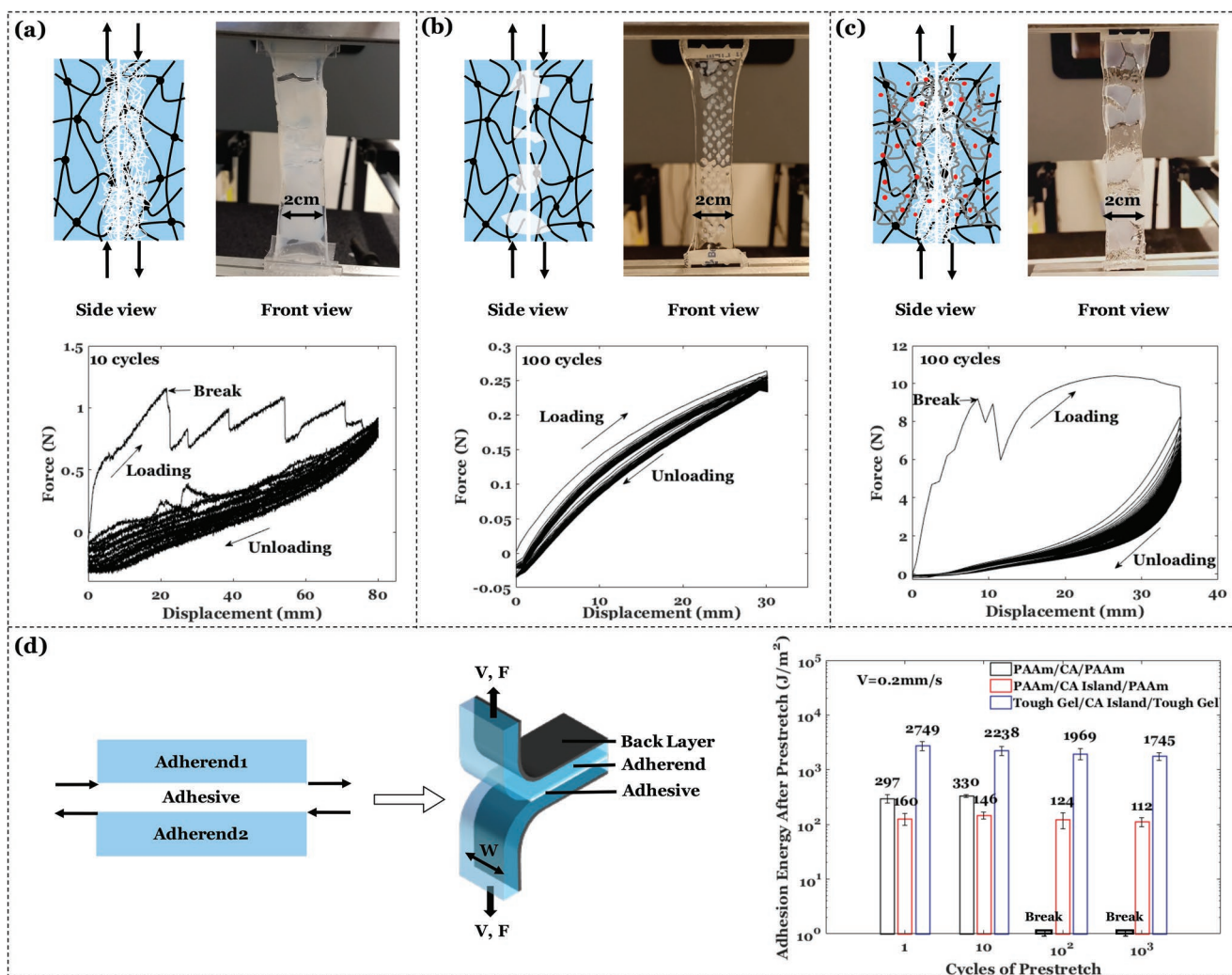


**Figure 6.** The stretchability of an adhered bilayer depends on the size of the rigid polymer. a) A bilayer formed by polyacrylamide hydrogels and continuous polycyanoacrylate layer is not stretchable. The bilayer fractures entirely within 10 cycles. b) A bilayer formed by polyacrylamide hydrogels and islands of polycyanoacrylate of  $\approx 1$  mm diameter is stretchable. The bilayer can be stretched for more than 100 cycles without fracture. c) A bilayer formed by calcium-alginate-polyacrylamide hydrogels and larger distributed polycyanoacrylate staples of  $\approx 1$ –2 cm diameter is stretchable. The bilayer can be stretched for more than 100 cycles without fracture. d) The characterization of stretchable adhesion. Samples are prescribed for different cycles of prestretch first, then intact samples after cyclic stretch are used to measure the adhesion energy by peel. Stretchable adhesions are measured for cases in (a)–(c) up to 1000 cycles. All samples are subject to cyclic stretch with an amplitude of 2. The stretching rate is fixed at  $0.25\text{ s}^{-1}$ . Adhesion is measured at  $V = 0.2\text{ mm s}^{-1}$ . Each data point with an error bar represents the mean and standard deviation of  $n \geq 3$  individual measured samples.

## 5. Staple a Hydrogel and an Elastomer Using a Diluted Cyanoacrylate

### 5.1. Diluted Cyanoacrylate

Wirthl et al. have shown that a cyanoacrylate-based glue diluted in an organic solvent can adhere hydrogels to an acrylic elastomer (very high bond tape (VHB), 3 M).<sup>[36]</sup> These authors have reported high adhesion energy, stretchability, and transparency. We speculate that these results are achieved through islands of glassy polycyanoacrylate of a size below the wavelength of light. For example, after the diluted cyanoacrylate is spin-coated or brushed on the surface of an adherend, cyanoacrylate may precipitate out, polymerize, and aggregate into small glassy islands. Direct observation of the glassy islands is lacking, and we are

uncertain if the mechanism proposed here is indeed responsible for the original finding of tough and stretchable adhesion.

When trying to repeat their experiments, we find a difficulty. We mix a commercial cyanoacrylate glue (KG-585 (Krazy glue) or Loctite 406 (Henkel)) in an organic solvent reported in the original paper (trimethylpentane, octadecene, or paraffin oil). After mixing, cyanoacrylate precipitates quickly, the amount of dissociation is difficult to control, and the timing to apply this mixture dramatically affects the adhesion. We rarely achieve a transparent interface with tough adhesion by this way. To enhance the stability of the mixture, we mix a commercial formulation of ethyl-cyanoacrylate in ethyl-acetate.<sup>[58]</sup> The mixture shows good solubility, and no precipitates are visible even after 1 h (Figure 7a). The dilution is prescribed by the volume ratio of the ethyl-cyanoacrylate formulation and ethyl-acetate.



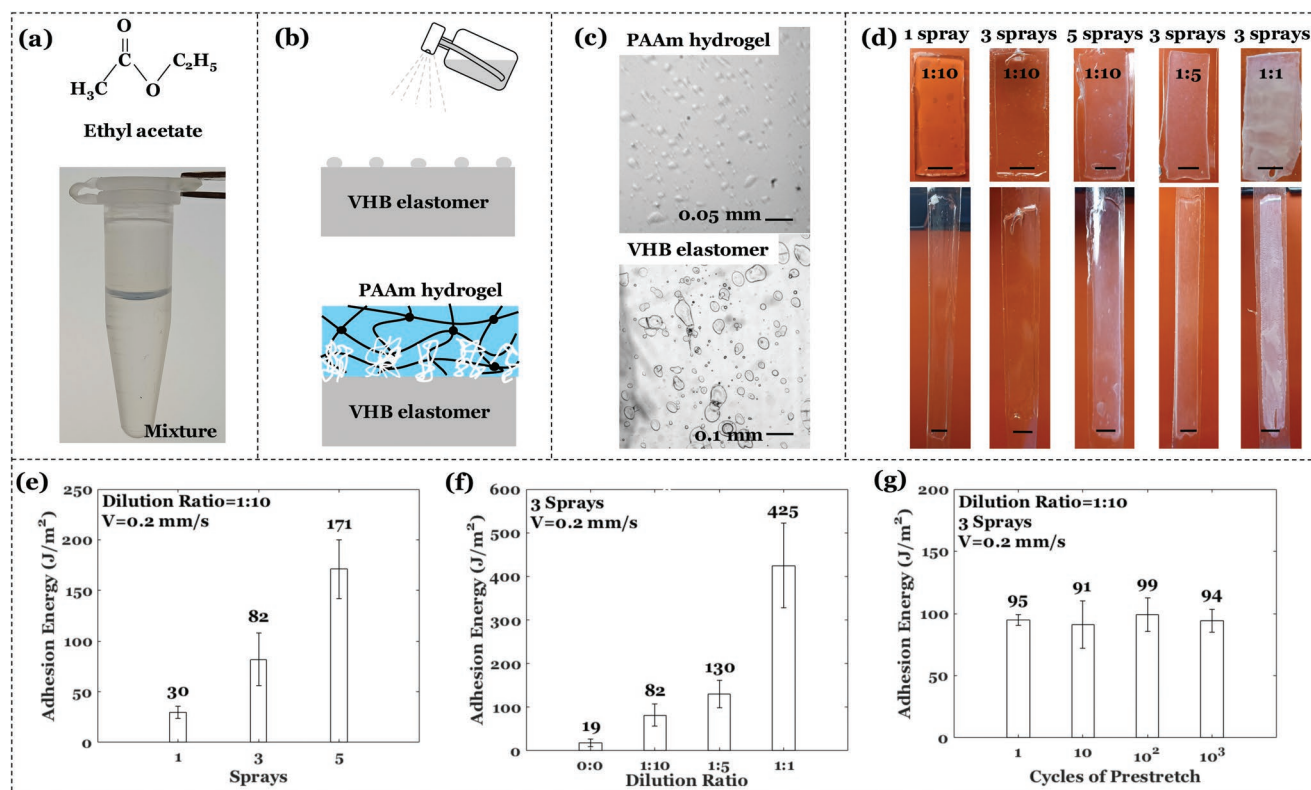


**Figure 7.** The formation and adhesion of molecular staples through diluted adhesive. a) The ethyl-cyanoacrylate formulation fully dissolves in ethyl acetate after mixing. No phase separation is observed in all dilution ratios. b) The small droplets of mixed solution are sprayed on the VHB elastomer. After spray, the polyacrylamide hydrogel is pressed on the top to form adhesion. c) After spray, the surfaces of polyacrylamide hydrogel (top) and VHB elastomer (bottom) are observed under a microscope. The images are taken after three events of spray. d) The VHB elastomer and polyacrylamide hydrogel bilayer (top) shows better transparency by adhesive with more dilution and fewer sprays. The same samples are stretched to 100% strain (bottom). The scale bar is 10 mm. e) Adhesion energy between VHB elastomer and polyacrylamide hydrogels with different numbers of spray. f) Adhesion energy with three sprays of cyanoacrylate of different dilution ratios. 0:0 means no adhesive applied between adherends. g) Adhesion energy measured after various cycles of stretch with amplitude of 2 and rate of  $0.25 \text{ s}^{-1}$ . Each data point with an error bar represents the mean and standard deviation of  $n \geq 3$  individual measured sample.

## 5.2. Forming Islands of a Hard Polymer by Spraying Drops of Liquid Precursor

In light of the proposed mechanism, we further modify the operation of adhesion to encourage the formation of small islands. Instead of spin-coating and brush, we spray the 1:10 mixture on the VHB elastomer and the polyacrylamide hydrogel (Figure 7b). We then observe the glassy islands in a microscope. By one event of spray, the individual glassy islands on the VHB elastomer are relatively uniform ( $\approx 10 \mu\text{m}$  on average). Multiple events of spray cause distributed size of 5–100  $\mu\text{m}$  (Figure 7c). Since the size of the islands is much smaller than the flaw sensitivity length, the adhered materials remain stretchable. More dilution and fewer sprays lead to more transparent bilayers (Figure 7d). Furthermore, the size control of molecular staples at even smaller length scale (e.g., nanometer) is possible, which can maintain tough adhesion and high stretchability, yet providing an optically transparent interface. This is beyond the scope of the current work.

In comparison to printing macroscopic glassy islands, spraying diluted adhesive not only reduces the size of glassy islands, but also enhances the transparency of interface,

making it feasible to the application of large scale integration of soft materials. The transparent interface allows light to travel through and may enable certain optical devices. The spraying method is limited by the rheology of the adhesive liquid. Viscous or shear-thickening adhesives are hard to be sprayed directly. The size of sprayed islands is unlikely to be specifically controlled, and the adhesive layer may not be uniform.

The size range and geometry of sprayed islands are affected by the outlet size of spray bottle, the distance between the spray bottle and adherends, the quantity of spray, and the dilution ratio. In practice, smaller outlet gives smaller staples, closer distance of spray gives higher density of staples to aggregate into larger islands. The aggregation of islands also increases with the applied contact force. More sprays and a higher dilution ratio lead to easier aggregation of large islands. In experiments, the spray bottle has an outlet size of  $\approx 100 \mu\text{m}$ , fixed in a distance of 10 cm from the adherends. The weight applied on the bilayer is 500 g. By fixing these, we investigate the effects of spray quantity and dilution ratio on adhesion in Section 5.3. So long as the size of islands is beyond the mesh size of the adherends and the distribution of islands is uniform, tough adhesion can be achieved.



### 5.3. Effect of Dilution on Adhesion Energy

We measure adhesion energies between VHB elastomer and polyacrylamide hydrogel with different numbers of spray (Figure 7e). We apply 1 to 5 sprays of the 1:10 diluted cyanoacrylate on the VHB elastomer and cover the polyacrylamide hydrogel on top with a constant weight. The adhesion energy increases with the number of spray. More sprays give more aggregation of glassy islands of larger size. 1–3 sprays lead to an interfacial fracture, while more sprays lead to a cohesive fracture.

We also record adhesion energies with 3 sprays of different dilution ratios of 1:1, 1:5, and 1:10 (Figure 7f). The adhesion energy decreases with the increasing degree of dilution, which is possibly due to the reduction of available molecular staples at the interface. A high dilution (1:10) leads to an interfacial fracture, while a low dilution (1:5) leads to a cohesive fracture in the polyacrylamide hydrogel. For a diluted adhesive, a higher dilution ratio possibly increases the molecular weight or chain length of the formed polycyanoacrylate. Here we do not characterize the detailed molecular structure of the final product. Nevertheless, the diluted cyanoacrylate does succeed to aggregate into glassy staples and provide efficient adhesion in the experiment. The adhesion energy is still high when the dilution ratio is 1:10 (Figure 7f).

The adhesion by spray-formed staples is stretchable and remains tough after many cycles of stretch (Figure 7g). After 1000 cyclic stretches with amplitude of 2 and rate of  $0.25 \text{ s}^{-1}$ , the adhesion of bilayer keeps at  $\approx 90 \text{ J m}^{-2}$ .

### 5.4. Interaction between Polycyanoacrylate and Elastomer

We have presented evidence that polycyanoacrylate forms topological entanglement with hydrogels. However, we are uncertain about the interaction between the polycyanoacrylate and VHB elastomer. In principle, polycyanoacrylate and an elastomer may form topological entanglement, densely packed noncovalent bonds, or covalently interlinks. The chemistry of VHB is proprietary, and a characterization of the interaction between polycyanoacrylate and VHB is beyond our capability. We further try to use cyanoacrylate to adhere PDMS and other soft materials (Table 1). Cyanoacrylate weakly adhere intact PDMS to PDMS, VHB, or high-water-content polyacrylamide hydrogel. These results indicate weak interaction between polycyanoacrylate and

**Table 1.** The adhesion energy by a continuous layer of polycyanoacrylate formed in situ between several pairs of soft materials. The peel velocity is  $V = 0.2 \text{ mm s}^{-1}$ . Adhesion energies between elastomer pairs are the average results of three individual measurements ( $n = 3$ ), and the maximum standard deviation is less than  $10 \text{ J m}^{-2}$ .

$[J \text{ m}^{-2}]$	PDMS	Rubbed PDMS	Polyacrylamide <sup>a)</sup>
VHB	6	26	400–500
PDMS	3	15	10–20
Rubbed PDMS	15	30	260–400

<sup>a)</sup>For polyacrylamide-elastomer pairs, adhesion energies are shown in the range of three individual measurements.

PDMS, because the wettability of cyanoacrylate on the PDMS surface is poor compared to the VHB elastomer. We then rub PDMS using a 1000-grit sandpaper, and measure the adhesion energy between the rubbed PDMS and other soft materials by polycyanoacrylate. The adhesion between two pieces of rubbed PDMS is still low. However, the adhesion between the rubbed PDMS and polyacrylamide hydrogel is dramatically enhanced. Surface roughness of the elastomer may have enabled mechanical interlocking between PDMS and polycyanoacrylate.

Though creating isolated adhesive islands is primarily designed to bond soft materials, it is applicable to bond a pair of soft and hard materials as well. The deformation of the soft-hard bilayer is limited by the harder adherend. In addition to some elastomers, other hard materials, such as metals, oxides, ceramics, and plastics, can also bond to hydrogels-like soft materials by forming the adhesive islands, as long as the liquid adhesives can well wet the surfaces of these materials. For materials with a lower surface energy compared to adhesives, such as polypropylene, polyethylene, and PDMS compared to cyanoacrylates, chemical or physical pretreatment of material surfaces are usually conducted to enhance the wettability of adhesive droplets before bonding. During the formation of adhesive islands, the specific interaction between islands and soft or hard adherends depends on the permeability of liquid adhesives in adherends. For nonpermeable adherends like metals, oxides, and surface-treated plastics, the liquid adhesives form glassy islands that have the densely packed noncovalent interaction with adherend surfaces. For permeable materials, such as gels, some elastomers, and microporous rigid materials, the liquid adhesives may diffuse or be absorbed into the materials at a certain depth, in situ polymerize or precipitate, and then molecularly staple or interpenetrate with them.

## 6. Concluding Remarks

Among various methods of tough and stretchable adhesion between soft materials, molecular staples made of a hard polymer have several advantages. (1) The molecular staples form easily by cracking a continuous layer, printing drops of a liquid precursor, or spraying drops of the precursor. Other possible operations of adhesion by molecular staples include spinning coat, brushing, spreading stable emulsion formed by microfluidics, and using micropattern technologies. (2) Molecular staples enable the use of existing adhesives to integrate soft materials. (3) Most available hard adhesives do not need special preparation of chemistry or treatment of the adherends. (4) The widely used hard adhesives enable tough adhesion between soft or hard adherends, through forming either topological entanglement within bulk, or densely packed noncovalent bonds at the interface. (5) The design principle of molecular staples is not limited to hydrogel–hydrogel and hydrogel–elastomer, but can also be extended to other material pairs such as tissue–tissue, tissue–hydrogel, tissue–elastomer, and elastomer–elastomer.

The effect of the chain length of polycyanoacrylate on the size of molecular staple and adhesion energy calls for further study. For example, for diluted adhesives, in situ polymerized long chains might give excessive aggregations of glassy phase resulting in larger staples. However, if the chains are too short,

there will be smaller staples than the mesh size of adherends, resulting in failure of adhesion. A method to control the chain length of in situ polymerized polymer is desired. Cyanoacrylate polymerizes instantly, the kinetics of stapling is thus hard to control, and the adhesion shows negligible time-dependence after the waiting time of 1 min. These facts make cyanoacrylate not a good example to study the kinetics. We can study a better adhesion system of formation of molecular staples by polymers of controlled length.

Molecular staples made by crystallites wait to be discovered. For example, crystallization can be easily formed between long alkyl groups or by hydrogen bonds in semicrystalline hydrogels.<sup>[59–62]</sup> The mechanical properties of semicrystalline hydrogels can be tuned by any sort of strong interaction to facilitate various applications.<sup>[61]</sup> Molecular staple can be achieved using semicrystalline polymers. When applied at the interface between two soft materials, an aqueous solution of semicrystalline polymers diffuse into the adherend, in situ form crystallites, topologically entangled with adherend networks. This method will encourage another large group of polymers as tough and stretchable adhesives.

We have demonstrated tough and stretchable adhesion between polycyanoacrylate and elastomer, but have not studied the chemistry and topology of their interaction. One possible way to figure out is to modify monomers with fluorescent indicator, and obtain a 3D confocal microscopic vision. If the size of molecular staple is in the nanometer scale, it may be possible to observe through electron microscopy. Understanding why polycyanoacrylate fails to adhere certain elastomers helps the design of a new class of instant adhesives for elastomers.

The molecular staples can be “unstapled” on-demand to enable reversible adhesion. For example, polycyanoacrylate molecular staples can be thermally detachable. The glassy staple melts when the ambient temperature becomes higher than its glass transition temperature ( $T_g$ ). Above  $T_g$ , the physically entangled chains of staple can be slowly disentangled by a relatively small load. The energy to break the noncovalent interaction and pull out the physical entangled chains is on the order of 1–10 J m<sup>-2</sup>.<sup>[53]</sup> A polycyanoacrylate with glass transition temperature above 100 °C is unsuitable for reversible adhesion for hydrogels,<sup>[47]</sup> but might be suitable for other adherends such as ionogels.<sup>[63]</sup> Some polycyanoacrylates have glass transition temperature below the boiling temperature of water, such as the anionic polymerized isobutyl  $\alpha$ -cyanoacrylate with  $T_g$  of 56 °C.<sup>[47]</sup> Debonding can also be induced by the degradation of covalent intrachain bonds in polycyanoacrylate under high temperature<sup>[64]</sup> or in biological environment.<sup>[65]</sup> Other hard polymers may find even more suitable temperature range to be thermally detachable, or chemical properties to be biodegradable. In addition, many other triggers are possible for reversible adhesion of specific hard polymers, including pH, light, salt, and other chemicals.

In summary, we have presented a design principle to integrate soft materials using hard polymers. An adhered bilayer can be as stretchable as the adherends themselves. The adhesion remains tough even after 1000 cycles of stretch in the plane of the interface. It is hoped that molecular staples will assist the invention and development of integrated soft materials.

## 7. Experimental Section

**Materials Preparation:** The PAAm hydrogel was synthesized by an aqueous solution of acrylamide (AAm, Sigma-Aldrich A8887) of 1.9 M, together with *N,N'*-methylenebis(acrylamide) (Sigma-Aldrich M7279) of 0.06 wt%, *N,N,N',N'*-tetramethylethylenediamine (Sigma-Aldrich T7024) of 0.25 wt%, and ammonium persulfate (Sigma-Aldrich 248614) of 0.42 wt% of the acrylamide monomer. The pH of the hydrogel was adjusted by dripping hydrochloric acid (Sigma-Aldrich 258148) in the precursor. Without specific notation, all the polyacrylamide hydrogels mentioned are in pH = 7. The precursor solution was completely mixed, degassed, and injected into glass molds of 2 cm wide, 5 cm long, and 1.5 mm thick. The samples were then stored at room temperature for more than 12 h for complete polymerization. To prepare the double-network calcium-alginate-polyacrylamide hydrogel, the same precursor of polyacrylamide was used. Sodium alginate (GMB, FMC Corporation) of 16.7 wt% and calcium sulfate dehydrate (Sigma-Aldrich C37771) of 3.2 wt% of the acrylamide monomer were added additionally. The operation follows the protocol of Sun et al.<sup>[56]</sup> KG-585 (Krazy glue) and Loctite 406 (Henkel) were used as cyanoacrylate-based commercial glues, of which the main component was ethyl-cyanoacrylate. To prepare a 30 mL alginate solution, alginic acid sodium salt ( $M_w \approx 120\,000$ – $190\,000$  Da, Sigma-Aldrich, 180947) of 0.9 g was dissolved in deionized water. The solution was vigorously mixed and sonicated in an ultrasonic bath at room temperature for 1 h. To prepare a 30 mL solution of cellulose, sodium hydroxide pellets (Macron) of 2.1 g, and urea powders (Sigma-Aldrich, U5128) of 3.6 g were directly dissolved in deionized water. The solution was precooled at –20 °C for 1 h before use. Afterward, cellulose powder (Sigma-Aldrich, 435236) of 0.6 g was added into the solution. The solution was vigorously mixed until becoming completely transparent. A commercial product Loctite Epoxy was used as the epoxy adhesive. Components A (epoxy resin) and B (cure agent) were mixed by a 1:1 volume ratio before use. To synthesize the PDMS elastomer, the precursor and crosslinker (Sylgard 184, Dow Corning) were mixed by a weight ratio of 20:1 and degassed for 2 min by a functional mixer (Thinky ARE-250). The mixture was poured into a rectangular acrylic mold with inner width of 2 cm and depth of 1.5 mm, and heated at 60 °C in a thermal chamber (Model 11E, Jeio Tech) for 24 h. A 1000-grit sandpaper (Sia Abrasive, Inc.) was used for rubbing the surface of PDMS.

**Adhesion Process:** Two pieces of hydrogels (2 cm wide, 5 cm long, 1.5 mm thick) were taken out from glass molds for adhesion. Adhesive liquids of 200  $\mu$ L were uniformly dripped on one piece of hydrogel and the other on top was immediately covered. An additional weight of 500 g was put on the adhered bilayers. After a prescribed period of time, the adhesion energy was measured by the peel test at different peel velocities  $V$ . Unless specifically mentioned, all the adhesion processes followed this protocol. All the samples were measured after 5 min except for the time dependent experiments.

**Molding Polydimethylsiloxane:** An acrylic sheet (1.5 mm thick, McMaster-Carr) was cut into a rectangular shape with width of 2 cm and length of 5 cm by a laser cutter (Helix 75W, Epilog). Another 1.5 mm thick rectangular frame with inner width of 3 cm and length of 6 cm was cut following the same process. These sheets were installed and adhered on a flat acrylic sheet by Krazy glue as the groove for the PDMS. The PDMS precursor and crosslinker (Sylgard 184, Dow Corning) were mixed by a weight ratio of 15:1 and degassed for 2 min by a functional mixer (Thinky ARE-250). The mixture was poured into the acrylic groove and heated to cure at 60 °C in a thermal chamber (Model 11E, Jeio Tech) for 4 h.

**Humidity Control:** Long-term experiments such as peel tests at slow speeds were done in a homemade humidity chamber of acrylic. Moisture in the chamber was supplied by a humidifier (HTJ-2003A, TLC Diagnostic Pty Ltd.) with a negative feedback control by a sensor (Hygrotherm, Zoo MED Laboratories, Inc.) to keep the relative humidity in chamber around the set value with an error of  $\pm 3\%$ .

**Casting Polycyanoacrylate and Polyacrylamide:** The PDMS molds were attached on a glass substrate, and a thin layer of Krazy glue was poured

into the PDMS mold to form the polycyanoacrylate. These filled molds were stored in a homemade acrylic chamber, and the chamber was stored inside a fume hood (Supreme Air LV, Kewaunee Scientific Co.) for three days to complete the polymerization of cyanoacrylate. The relative humidity measured by a humidity sensor (Taylor Hygrometer) in the chamber was 10%. After polymerization, the glassy polycyanoacrylate bonds the glass substrate tightly. The polyacrylamide precursor was poured on top of the glassy polycyanoacrylate until filling full of the PDMS mold. Another glass was used to seal the precursor on the top. The whole structure was kept at room temperature for 12 h for complete polymerization. To measure the adhesion of the casted polyacrylamide on polycyanoacrylate, the PDMS mold was removed after the polymerization.

**Peel Test:** Both 180° and 90° peel tests were performed on a tensile machine (Instron 5966) with a 100 N load cell (Instron 2530). The 180° peel test was for both the adhesion and fracture of hydrogels, and the 90° peel test was for the adhesion of casted hydrogels. For adhesion tests by the 180° peel, an initial crack of 1 cm was made at the front of sample by preserving a space without adhesion at the interface between two adherends during the preparation of adhesion. For the fracture test of polyacrylamide hydrogel, an initial crack of 1 cm long was prescribed during the polymerization. During the test, an inextensible polyester film was attached on the outward surface of each layer. The two adherends were gripped by the tensile machine at their precracked ends in the test (Figure 3a,b). To measure the adhesion of casted hydrogels, a 90° peel test fixture (Instron 2820-035) was used. An initial crack of 1 cm was made by a manual peel of the polyacrylamide hydrogel from the polycyanoacrylate film. The sample on the glass substrate was mounted on the fixture. Only the hydrogel was gripped (Figure 4b). The peel velocity for both peel tests is represented by  $V$  in Figure 3a,b and Figure 4b. Except for measuring the  $G$ - $V$  curves, the peel velocity is 0.2 mm s<sup>-1</sup> in all the rest experiments. For low-speed peel tests, the humidity was held at 95% by using the humidity chamber.

**Cyclic Test:** After the adhesion, a sample was cyclically stretched in the planar direction by the tensile machine (Instron 5966). The maximum uniaxial stretch is 2. The stretching rate is 0.25 s<sup>-1</sup>. For long-time cyclic tests, samples were stretched in the humidity chamber with a relative humidity held at 95%.

**Formation of Glassy Islands:** Toothpicks (Montopack, Hanamal Ltd.) with tip diameter of 0.5 mm were packed and adhered by Krazy glue to form a lattice of 2 cm wide and 5 cm long. Krazy glue was uniformly brushed on the top of the lattice. The lattice was then gently stamped on the surfaces of both adherends, the adherends were attached together quickly, and the bilayer was pressed with a 500 g weight for 5 min. The size of glassy islands formed in this way was measured to be about 1–2 mm. The size of printed islands mainly depends on the tip size of the lattice. Islands with a specific size or shape of particular interest were prepared by prescribing the corresponding tip of lattice in a wide range.

**Diluted Adhesive:** Commercial glues KG-585 (Krazy glue) or Loctite 406 (Henkel) were diluted in ethyl-acetate (Sigma-Aldrich 319902) of one, five, ten times the volume. After dilution, the mixture was sprayed on an acrylic elastomer VHB 4905 (3 M) by a fine mist glass spray (B071KX2KK6, Enslz) from a distance of 10 cm. A polyacrylamide hydrogel was immediately placed on top of the elastomer afterward, and pressed by a 500 g weight for 5 min.

**Test of Stretchable Adhesion:** After printing drops of a liquid precursor or spraying drops of the precursor, the adhered bilayer was subject to the prescribed cyclic test. After the cyclic test, the adhesion energy was measured using the 180° peel test.

**Microscopy:** Diluted cyanoacrylate-based glue (Loctite 406 (Henkel)) of 1:10 was sprayed for three times on a VHB elastomer and a polyacrylamide hydrogel. After 5 min, each of them was placed in the microscope (Apo Tome.2, ZEISS). The microscopic photos of the sample surface were captured by using the ZEISS software with automatic adjustment.

**Statistical Analysis:** The force–displacement curve for each individual test was plotted using Microsoft Excel, and the average force  $F_{ave}$  was calculated by averaging the data points at the plateau of the curve.  $F_{ave}$

was converted into the adhesion energy  $G$  by  $G = 2F_{ave}/W$ , where  $W$  is the width of each sample. Each data point with an error bar represents the mean and standard deviation of  $n \geq 3$  individual measured samples. The mean value and standard deviation are calculated using MATLAB (MathWorks).

**Video 1.** Peel of two polyacrylamide hydrogels adhered by a continuous layer of polycyanoacrylate at  $V = 0.2$  mm s<sup>-1</sup>. Played at the 8× speed.

**Video 2.** Two polyacrylamide hydrogels adhered by printed islands of polycyanoacrylate are subject to a cyclic stretch with amplitude of 2 and rate of 0.25 s<sup>-1</sup>. Played at the 1× speed.

**Video 3.** Two calcium-alginate-polyacrylamide hydrogels adhered by printed islands of polycyanoacrylate are subject to a cyclic stretch with amplitude of 2 and rate of 0.25 s<sup>-1</sup>. Played at the 2× speed.

**Video 4.** The peel of island-stapled polyacrylamide hydrogel bilayer at  $V = 0.2$  mm s<sup>-1</sup>. Played at the 8× speed.

## Supporting Information

Supporting Information is available from the Wiley Online Library or from the author.

## Acknowledgements

This work was supported by NSF MRSEC (DMR-14-20570).

## Conflict of Interest

The authors declare no conflict of interest.

## Keywords

glassy adhesives, molecular staples, soft materials, stretchable adhesions

Received: June 22, 2019

Revised: July 16, 2019

Published online:

- [1] S. V. Murphy, A. Atala, *Nat. Biotechnol.* **2014**, 32, 773.
- [2] J. Yang, R. Bai, B. Chen, Z. Suo, *Adv. Funct. Mater.* **2019**, 1901693.
- [3] D. Rus, M. T. Tolley, *Nature* **2015**, 521, 467.
- [4] S.-H. Ahn, K.-T. Lee, H.-J. Kim, R. Wu, J.-S. Kim, S.-H. Song, *Int. J. Precis. Eng. Manuf.* **2012**, 13, 631.
- [5] Z. Wang, C. Xiang, X. Yao, P. Le Floch, J. Mendez, Z. Suo, *Proc. Natl. Acad. Sci. USA* **2019**, 116, 5967.
- [6] R. L. Truby, J. A. Lewis, *Nature* **2016**, 540, 371.
- [7] P. Le Floch, X. Yao, Q. Liu, Z. Wang, G. Nian, Y. Sun, L. Jia, Z. Suo, *ACS Appl. Mater. Interfaces* **2017**, 9, 25542.
- [8] P. Le Floch, S. Meixuanzi, J. Tang, J. Liu, Z. Suo, *ACS Appl. Mater. Interfaces* **2018**, 10, 27333.
- [9] J. Li, A. Celiz, J. Yang, Q. Yang, I. Wamala, W. Whyte, B. Seo, N. Vasilyev, J. Vlassak, Z. Suo, *Science* **2017**, 357, 378.
- [10] L. Han, L. Yan, K. Wang, L. Fang, H. Zhang, Y. Tang, Y. Ding, L.-T. Weng, J. Xu, J. Weng, *NPG Asia Mater.* **2017**, 9, e372.
- [11] R. Dimatteo, N. J. Darling, T. Segura, *Adv. Drug Delivery Rev.* **2018**, 127, 167.
- [12] H. Hamed, S. Moradi, S. M. Hudson, A. E. Tonelli, *Carbohydr. Polym.* **2018**, 199, 445.
- [13] N. Noor, A. Shapira, R. Edri, I. Gal, L. Wertheim, T. Dvir, *Adv. Sci.* **2019**, 6, 1900344.

- [14] U. Mirsaidov, J. Scrimgeour, W. Timp, K. Beck, M. Mir, P. Matsudaira, G. Timp, *Lab Chip* **2008**, 8, 2174.
- [15] Y. Murakami, M. Yokoyama, T. Okano, H. Nishida, Y. Tomizawa, M. Endo, H. Kurosawa, *J. Biomed. Mater. Res., Part A* **2007**, 80A, 421.
- [16] G. M. Whitesides, *Angew. Chem., Int. Ed.* **2018**, 57, 4258.
- [17] H. R. Lee, C. C. Kim, J. Y. Sun, *Adv. Mater.* **2018**, 30, 1704403.
- [18] C. H. Yang, B. Chen, J. J. Lu, J. H. Yang, J. Zhou, Y. M. Chen, Z. Suo, *Extreme Mech. Lett.* **2015**, 3, 59.
- [19] C.-C. Kim, H.-H. Lee, K. H. Oh, J.-Y. Sun, *Science* **2016**, 353, 682.
- [20] C. Yang, Z. Suo, *Nat. Rev. Mater.* **2018**, 3, 125.
- [21] H. Yuk, B. Lu, X. Zhao, *Chem. Soc. Rev.* **2019**, 48, 1642.
- [22] B. C.-K. Tee, A. Chortos, A. Berndt, A. K. Nguyen, A. Tom, A. McGuire, Z. C. Lin, K. Tien, W.-G. Bae, H. Wang, *Science* **2015**, 350, 313.
- [23] S. Lim, D. Son, J. Kim, Y. B. Lee, J. K. Song, S. Choi, D. J. Lee, J. H. Kim, M. Lee, T. Hyeon, *Adv. Funct. Mater.* **2015**, 25, 375.
- [24] J.-W. Jeong, G. Shin, S. I. Park, K. J. Yu, L. Xu, J. A. Rogers, *Neuron* **2015**, 86, 175.
- [25] I. Skeist, *Handbook of Adhesives*, Springer US, Van Nostrand Reinhold, New York, NY **1990**, <https://doi.org/10.1007/978-1-4613-0671-9>.
- [26] H. Ablat, I. Povey, R. O'Kane, S. Cahill, S. D. Elliott, *Polym. Chem.* **2016**, 7, 3236.
- [27] H. Yuk, T. Zhang, S. Lin, G. A. Parada, X. Zhao, *Nat. Mater.* **2016**, 15, 190.
- [28] H. Yuk, T. Zhang, G. A. Parada, X. Liu, X. Zhao, *Nat. Commun.* **2016**, 7, 12028.
- [29] Q. Liu, G. Nian, C. Yang, S. Qu, Z. Suo, *Nat. Commun.* **2018**, 9, 846.
- [30] H. Yang, C. Li, M. Yang, Y. Pan, Q. Yin, J. Tang, H. J. Qi, Z. Suo, *Adv. Funct. Mater.* **2019**, 29, 1901721.
- [31] J. Yang, R. Bai, J. Li, C. H. Yang, X. Yao, Q. Liu, J. Vlassak, D. Mooney, Z. Suo, *ACS Appl. Mater. Interfaces* **2019**, <https://doi.org/10.1021/acsami.9b07522>.
- [32] J. Yang, R. Bai, Z. Suo, *Adv. Mater.* **2018**, 30, 1800671.
- [33] Y. Gao, K. Wu, Z. Suo, *Adv. Mater.* **2018**, 31, 1806948.
- [34] R. J. Chang, A. Gent, *J. Polym. Sci., Polym. Phys. Ed.* **1981**, 19, 1635.
- [35] A. Gent, R. Tobias, *J. Polym. Sci., Polym. Phys. Ed.* **1984**, 22, 1483.
- [36] D. Wirthl, R. Pichler, M. Drack, G. Kettlguber, R. Moser, R. Gerstmayr, F. Hartmann, E. Bradt, R. Kaltseis, C. M. Siket, *Sci. Adv.* **2017**, 3, e1700053.
- [37] D. M. Toriumi, K. O'grady, D. Desai, A. Bagal, *Plast. Reconstr. Surg.* **1998**, 102, 2209.
- [38] A. T. Trott, *JAMA, J. Am. Med. Assoc.* **1997**, 277, 1559.
- [39] P. A. Leggat, D. R. Smith, U. Kedjarune, *ANZ J. Surg.* **2007**, 77, 209.
- [40] D. M. Toriumi, W. F. Raslan, M. Friedman, M. E. Tardy, *Arch. Otolaryngol., Head Neck Surg.* **1990**, 116, 546.
- [41] H. Vinters, K. Galil, M. Lundie, J. Kaufmann, *Neuroradiology* **1985**, 27, 279.
- [42] L. Montanaro, C. Arciola, E. Cenni, G. Ciapetti, F. Savioli, F. Filippini, L. Barsanti, *Biomaterials* **2000**, 22, 59.
- [43] J. L. Down, *Stud. Conserv.* **2001**, 46, 35.
- [44] K. L. Mittal, *Progress in Adhesion and Adhesives*, John Wiley & Sons, Inc., Hoboken, New Jersey **2015**, <https://www.wiley.com/en-us/Progress+in+Adhesion+and+Adhesives-p-9781119162193>.
- [45] C. Limouzin, A. Caviggia, F. Ganachaud, P. Hémerly, *Macromolecules* **2003**, 36, 667.
- [46] G. Henrici-Olivé, S. Olivé, *Chemistry*, Springer, Berlin, Heidelberg **1979**, p. 123, [https://doi.org/10.1007/3-540-09442-3\\_6](https://doi.org/10.1007/3-540-09442-3_6).
- [47] R. Kulkarni, H. Porter, F. Leonard, *J. Appl. Polym. Sci.* **1973**, 17, 3509.
- [48] H. Yu, Z. Suo, *J. Mech. Phys. Solids* **1998**, 46, 829.
- [49] C. Chen, Z. Wang, Z. Suo, *Extreme Mech. Lett.* **2017**, 10, 50.
- [50] R. Bai, B. Chen, J. Yang, Z. Suo, *J. Mech. Phys. Solids* **2019**, 125, 749.
- [51] A. Gent, S. M. Lai, *J. Polym. Sci., Part B: Polym. Phys.* **1994**, 32, 1543.
- [52] T. Baumberger, C. Caroli, D. Martina, *Eur. Phys. J. E* **2006**, 21, 81.
- [53] T. Baumberger, C. Caroli, D. Martina, *Nat. Mater.* **2006**, 5, 552.
- [54] R. Bai, J. Yang, Z. Suo, *Eur. J. Mech.: A/Solids* **2019**, 74, 337.
- [55] R. Jenkins, L. Karre, *J. Appl. Polym. Sci.* **1966**, 10, 303.
- [56] J.-Y. Sun, X. Zhao, W. R. Illeperuma, O. Chaudhuri, K. H. Oh, D. J. Mooney, J. J. Vlassak, Z. Suo, *Nature* **2012**, 489, 133.
- [57] R. Bai, Q. Yang, J. Tang, X. P. Morelle, J. Vlassak, Z. Suo, *Extreme Mech. Lett.* **2017**, 15, 91.
- [58] J. Tang, Z. Tong, Y. Xia, M. Liu, Z. Lv, Y. Gao, T. Lu, S. Xie, Y. Pei, D. Fang, *J. Mater. Chem. B* **2018**, 6, 2713.
- [59] J. Li, Z. Suo, J. J. Vlassak, *J. Mater. Chem. B* **2014**, 2, 6708.
- [60] H. Zhang, D. Han, Q. Yan, D. Fortin, H. Xia, Y. Zhao, *J. Mater. Chem. A* **2014**, 2, 13373.
- [61] C. Bilici, S. Ide, O. Okay, *Macromolecules* **2017**, 50, 3647.
- [62] A. Matsuda, J. i. Sato, H. Yasunaga, Y. Osada, *Macromolecules* **1994**, 27, 7695.
- [63] B. Chen, J. J. Lu, C. H. Yang, J. H. Yang, J. Zhou, Y. M. Chen, Z. Suo, *ACS Appl. Mater. Interfaces* **2014**, 6, 7840.
- [64] M. G. Han, S. Kim, S. X. Liu, *Polym. Degrad. Stab.* **2008**, 93, 1243.
- [65] D. Hee Park, S. Bum Kim, K. D. Ahn, E. Yong Kim, Y. Jun Kim, D. Keun Han, *J. Appl. Polym. Sci.* **2003**, 89, 3272.